Polyoxymethylene Orientation by Equal-Channel Multiple Angular Extrusion

V. A. Beloshenko, V. N. Varyukhin, A. V. Voznyak, Yu V. Voznyak

Donetsk Institute for Physics and Engineering, National Academy of Sciences of Ukraine, 83114 Donetsk, Ukraine

Received 26 November 2011; accepted 5 February 2012
DOI 10.1002/app.36971
Published online in Wiley Online Library (wileyonlinelibrary.com).

ABSTRACT: The effect of conditions and routes of deformation in the course of equal-channel multiple-angular extrusion (ECMAE) on physical and mechanical properties of polyoxymethylene (POM) have been studied. As deformation routes, Route C (shear planes are parallel, and the simple shear direction of every deformation zone is changed through 180°) and Route E (shear planes are turned through ±45° around the extrusion axis and the normal to the axis, and simple shear direction is changed through 180° or ±90° with respect to the deformation zone) were selected. It has been shown that ECMAE provides the increase of modulus of elasticity E more than twice, tensile strength σ_T increases in four times. At the same time, strain at break ε_b is reduced by 1.5%. The value of the achieved effects depends on the accumulated deformation and the selected deformation route. The best set of physical and mechanical characteristics was observed in the case of Route E. According to SEM data, Route C results in partial pore healing and E provides total pore healing both in longitudinal and transversal direction. The observed effects are related to orientation order formation, increase of cristallinity degree and reduction of structure imperfection of extrudates. © 2012 Wiley Periodicals, Inc. J Appl Polym Sci 000: 000–000, 2012

Key words: polyoxymethylene; equal-channel multiple angular extrusion; processing route

INTRODUCTION

Solid-phase molecular orientation allows significant improvement of strength characteristics of semicrystalline polymers and production of fibers, films, rods, plates, and tubes with a set of high properties. This process is realized with using of tensile drawing, die-drawing, roll and roll-drawing, ram and hydrostatic extrusion, twist extrusion, etc.[1,2]

The whole variety of the methods of solid-phase molecular orientation can be divided into two groups. The first group includes methods based on polymer billet deformation accompanied by form change (stretching). The second group unites processes not related to form and size change, being based on simple shear. The most far-famed is equal channel angular extrusion (ECAE).[2,3] In the course of ECAE, a billet is pressed through two channels of equal cross-sections intercepting usually at 90°. It is shown in literatures,[4–9] that ECAE forms oriented lamellar or microfibrillar structure in semicrystalline polymers. Orientation degree and the achieved level of physical and mechanical properties are determined by the value of accumulated deformation (the number of passes through intersecting channels) and the selected deformation route. They include[3]: Route A when the orientation of the billet remains the same at the every pass; Route B when the billet is rotated 90° clockwise and counterclockwise alternatively around the longitudinal axis after every extrusion cycle; Route C when the billet is rotated 180° around the longitudinal axis after every extrusion cycle; Route D when the billet is rotated 90° clockwise around the longitudinal axis after every extrusion cycle.

A modified variant of ECAE is equal-channel multiple-angular extrusion (ECMAE) that implies presence of several zones of shear deformation within one device, in contrast to ECAE.[2] That is why accumulation of high plastic deformation per one cycle takes place and at the same time, high homogeneity of deformation distribution through billet section is provided.[10–13] A specific feature of ECMAE is possibility of realization of combination of different deformation routes during one cycle of the process.

Earlier we have established for polyamide-6, polyethylene of high and low density, polytetrafluorethylene that ECMAE is an effective method of structure modification of semicrystalline polymers enhancing the rigidity and the strength of the mentioned material with plasticity conserved at a high level.[11–13] Besides, ECMAE provides low anisotropy of the properties at longitudinal and cross sections of the produced billets.

The structure and the properties of the oriented polyoxymethylene were studied in a number of

Correspondence to: V. A. Beloshenko (bel@hpress.fti.ac.donetsk.ua).

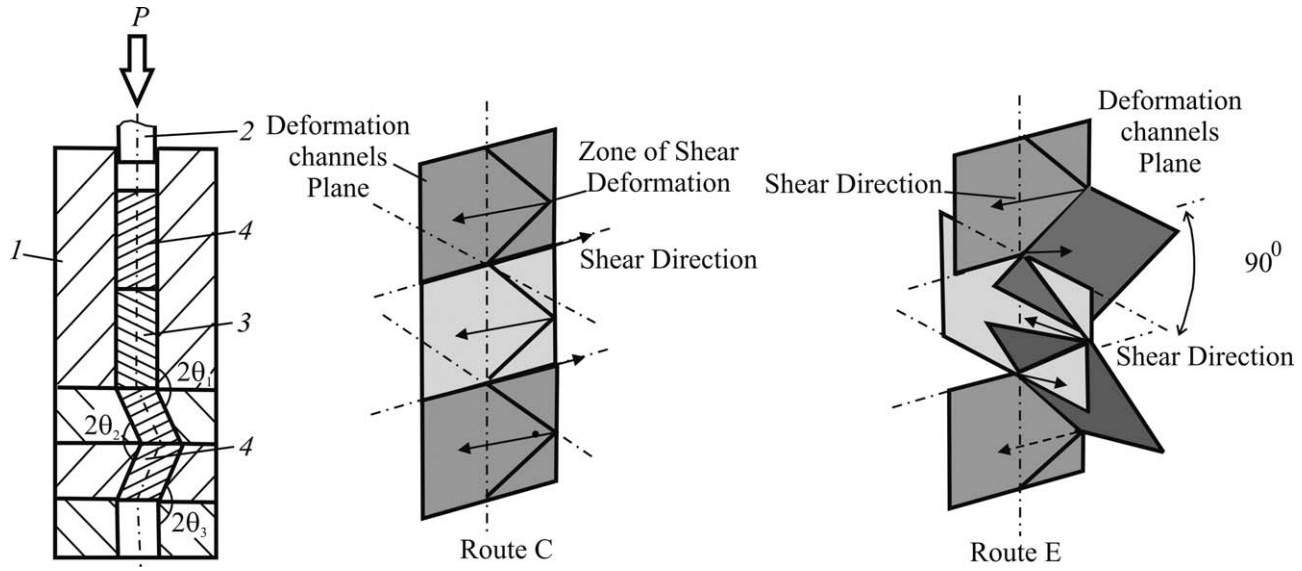

Figure 1 Scheme of ECMAE process: 1—die, 2—punch, 3—polymeric billet, 4—sacrified billets.

works.[14–17] They give evidences that the results may differ essentially depending on the selected deformation scheme. In particular, this fact was observed in the course of solid-phase processing with using of die-drawn, hydrostatic extrusion, rolling with side constrains.[16,17] The present article studies evolution of the structure and the properties of POM at ECMAE with varied control conditions.

EXPERIMENT

Figure 1 demonstrates ECMAE scheme. A polymer billet is pressed through a device consisting of several pairs of channels of the same diameter intersecting at varied angles θ_i. The inlet and outlet channels were made vertically coaxial to keep the billet pointing to the right direction. Inclined channel pairs form so-called knee. Position of the knee can be changed by turning the channels around the vertical axis. The control over the position of the shearing plane in the space guarantees different variants of deformation spatial development. Figure 1 shows also the positions of deformation channels plane used in the work. They support the shear planes are parallel, and the simple shear direction of every deformation zone is changed through 180° (Route C) or shear planes are turned through ±45° around the extrusion axis and the normal to the axis, and simple shear direction is changed through 180° or ±90° with respect to the deformation zone (we call it Route E). The extrusion was carried out at the temperatures of 363, 383, 403, 418, and 428 K. For that, the incoming billet and technological equipment were preliminary heated up to the mentioned temperatures. Temperature and extrusion pressure control was done with using universal measuring and controlling device TRM-151-01, Owen, Ukraine. Observational temperature accuracy was 0.1 K, the pressure accuracy was $1 \cdot 10^{-4}$ MPa. The temperature of the deforming block within the container was maintained with accuracy of ±1K.

For the attaining of a uniform deformation over extrudate length and avoiding the bending of extrudate ends, we used sacrified billets placed ahead of and behind the studied object. An incoming billet acted as the upper sacrified billet when a series of extrudates was produced.

The plastic deformation intensity $\Delta\Gamma_i$ and the value of accumulated deformation ε were determined by the formulae:[11]

$$\Delta\Gamma_i = 2ctg\theta_i \tag{1}$$

$$\varepsilon = 2\sum_{i=1}^{n} \frac{ctg\theta_i}{\sqrt{3}} \tag{2}$$

where θ_i is the half-angle of channel intersection, n is the number of channel-intersection angles. The extrusion rate was about 0.6×10^{-3}m s^{-1}, and the deformation intensity $\Delta\Gamma_1 = 0.83$, that corresponded to optimum conditions of the process.[10,11]

Polyoxymethylene TECAFORM AH, ENSINGER was the object of our research. The melting temperature of POM was 438 K. The billets of the required size (the diameter of 15 mm, the length of 50 mm) were cut from cylindrical rods 16 mm in diameter.

We chose the method of microhardness H measurement as one of the basic investigation methods. This allowed us not only to simplify the mechanical testing but also to obtain information on the uniformity of the strain over a section of the extrudates.

Because the microhardness of polymers is proportional to the yield strength σ_y,[18] the microhardness distribution suggests the strain uniformity. Microhardness H was determined using a microhardness tester of the PMT-3 type. The indenter was a tetrahedral diamond pyramid with the vertex angle of 136°. The pyramid was fluently pressed into the sample at the loading of 0.5 N. The value of microhardness H was estimated by the formula $H = 0.1854\frac{F}{d^2}$, where F—loading, N; d—diagonal of the indentation; $d^2/1.854$—area of the lateral surface of produced pyramidal indentation. For H, the relative error was not higher than 5%. The uniformity of H distribution over the sections of extrudates was estimated by value of dispersion D_H determined by the formula:

$$D_H = \sqrt{\frac{1}{n(n-1)}\sum_{i-1}^{n}(\bar{H} - H_i)^2}, \quad (3)$$

where n—number of measurements, H_i—result of an individual measurement of microhardness value, $\bar{H}$—average microhardness value. The value of microhardness anisotropy ΔH characterizing the difference in the strength properties in longitudinal and transverse sections of extrudates was estimated by the formula[19]:

$$\Delta H = 1 - \frac{\bar{H}^{\perp}}{\bar{H}^{||}}, \quad (4)$$

where $\bar{H}^{\perp}$, $\bar{H}^{||}$ —average values of microhardness in cross and longitudinal sections of extrudates, respectively.

The dumb-bell shaped specimens (head size, diameter 10 mm; length, 10 mm; working-part size, diameter, 5 mm; length, 30 mm) were subjected to tensile tests. The specimens were cut along the direction of extrusion. The supporting platforms travelled at a velocity of 10 mm min^{-1}. The average values of yield strength σ_y, tensile strength σ_T, modulus of elasticity E, yield strain ε_y, strain at break ε_b and standard deviations were determined from testing five specimens of each sample.

The density of specimens ρ was determined by hydrostatic weighing (a balance of the AX200 type, Shimadzu). The volume degree of crystallinity (χ_c^{ρ}) was calculated using the following relationship:

$$\chi_c^{\rho} = (\rho - \rho_a)/(\rho_c - \rho_a), \quad (5)$$

where ρ_a and ρ_c are the densities of polymer amorphous and crystalline phases, respectively (for POM, ρ_a =1.25, ρ_c =1.50 g cm^{-3}).

The differential scanning calorimetry (DSC) was performed using a thermoanalytical complex DuPont 9900. The heating rate was equal to 20° min^{-1}, the weight mass—15 mg. Enthalpy of fusion, ΔH_f, was determined by integrating the area under the baseline correct thermogram. Percentage crystallinity χ_c^{DSC} was calculated from the ratio of $\Delta H_f / \Delta H_{f\ 100\%}$, where $\Delta H_{f\ 100\%}$ is the enthalpy of fusion for a fully crystalline polymer (for POM, $\Delta H_{f\ 100\%}$=326 J g^{-1}).[20]

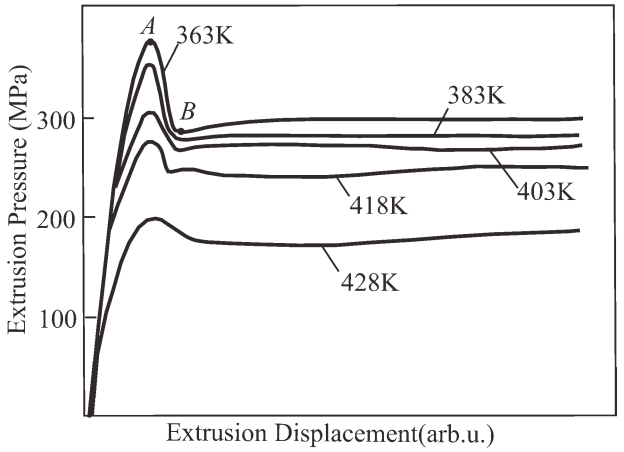

Figure 2 Effect of extrusion temperature on the dependence extrusion pressure—extrusion displacement. Route E, $\varepsilon = 4.4$.

For the determination of the thickness of crystalline stem l_c, the Gibbs-Thomson equations was used:

$$l_c = \frac{2\sigma_e T_m^0}{\Delta h_f (T_m^0 - T_m)} \quad (6)$$

where σ_e is the lamellar basal surface free energy (for POM, σ_e =0.125 J/m^2), Δh_f is the heat of fusion per unit volume (for POM, $\Delta h_f = 380 \cdot 10^6$ J/m^3), $T_m{}^0$ is the equilibrium melting temperature (for POM, $T_m{}^0$=473 K).[20]

Scanning electron microscopy (SEM) was implemented by using a JEOL JSM-6490 instrument at an accelerating voltage of 5 kV. A conducting layer (25- to 30-μm-thick golden layer) was applied to surface under investigation by cathode sputtering method. The photographs were taken of the surfaces of cross and longitudinal spallings of original samples and extrudates. The spalling was made at the liquid nitrogen temperature.

RESULTS AND DISCUSSION

The main factors determining the character of ECMAE process are deformation intensity (the value of channel intersection angle), accumulated deformation, processing route, the temperature of the billet, and the rate of its deformation.

Figure 2 presents typical relations of extrusion pressure and extrusion displacement, corresponding to ECMAE along Route E at varied extrusion temperature. The initial stage of extrusion is

TABLE I
Influence of ECMAE on Maximum Extrusion Pressure and Microhardness of POM

Routes of deformation	Accumulated strain values	Maximum extrusion pressure, MPa	Microhardness, in cross (longitudinal) sections, MPA	Microhardness anisotropy	Dispersion in microhardness
Initial	0	–	132 (133)	0.01	0.50
Route C	4.4	375	277 (322)	0.14	1.27
	6.7	603	317 (367)	0.14	1.09
	9.1	1070	320 (368)	0.13	1.01
Route E	4.4	310	395 (434)	0.09	1.07
	6.7	585	410 (445)	0.08	1.05
	9.1	890	440 (475)	0.07	0.97
	11.4	1150	448 (477)	0.06	0.95

characterized by increasing pressure of extrusion (the material is adapted to the angle between matrix channels). As soon as the front end of the billet entirely passes the last deforming channel (Point A), the loading becomes constant because the same volume of the material is exposed to and the process enters the stable stage. The observed succeeding reduction of extrusion pressure value (Point B) may be attributed to strain softening phenomenon in polymers, to the self-heating effect, or both.[21] Extrusion pressure for POM becomes almost constant after deformation stabilization. The maximum extrusion pressure P_m is reduced as the extrusion temperature increases. Analogous behavior of extrusion pressure takes place also in the case of Route C, but the value of the maximum pressure is higher (Table I). The difference of the absolute values of P_m for varied deformation routes can be connected with realized Bauschinger's effect,[22] i.e., the reduction of plastic deformation resistance at alternation of loading sign determined by the residual stresses that collide with the operating stress at the loading sign change and cause its reduction. Here the effect is significantly weakened at multiple cycle loadings. As Route C implies alternating-sign deformation in the same plane, the weakening of Bauschinger's effect will be stronger than in the case of Route E at the same deformation degree because Route E implements alternating-sign deformation in different planes.

With increase in the extrusion temperature T_e, extreme change of $\bar{H}$ was observed at the both deformation routes (Fig. 3), that was characteristic of solid-phase orientation of semicrystalline polymers, being explained by competition of strengthening processes determined by formation of oriented structure and softening caused by thermo-activated relaxation of oriented polymer chains. The behavior of extrudate density ρ is correlated within certain limits with the change of microhardness (Fig. 3). Here extreme character of $\rho(T_e)$ takes place, too. The maximum values of $\bar{H}$ and ρ are achieved at $T_e = 403$ K, so this temperature was selected as the optimum one for further investigations.

It is well-known that the deformation route is the most important parameter of ECAE process.[3] Its effect on the character of the formed microstructure and the properties of the crystallized polymers was studied in literatures.[5,23–26] It was shown there that in the case of Route A, a transition from the initial spherulitic structure to micro- and macrofibrillar one oriented along the shear direction is observed. In the case of Route C, each even extrusion cycle demonstrated off-orientation of macrofibrils followed by their thickening and partial renewal of spherulitic structure. Formation of such structures results in pronounced anisotropy of mechanical properties measured in varied directions about extrudate axis (Route A) or in more balanced mechanical properties in the case of Route C with less explicit difference in longitudinal and transversal directions.

Because of sign-alternating deformation character, ECMAE realizes mode of deformation corresponding to deformation along Route C or combination of varied deformation routes during one cycle of the process. The present work includes the case when simple shear direction being located in shear planes oriented at an angle of 45° to the extrusion axis and the normal to the axis or in shear planes located at an angle of 90° to the extrusion axis (Route E, Fig. 1).

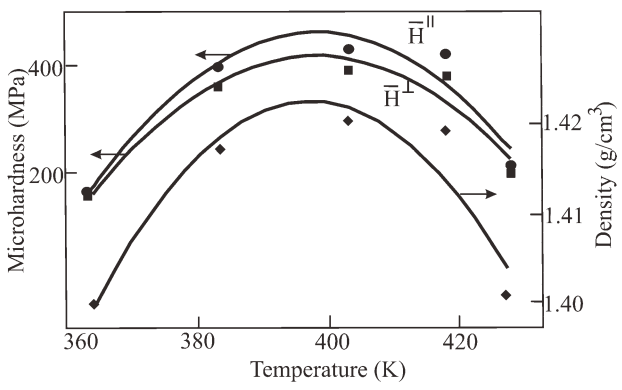

Figure 3 Dependences of the mean values of POM extrudates microhardness and density on ECMAE temperature. Route E, ε = 4.4.

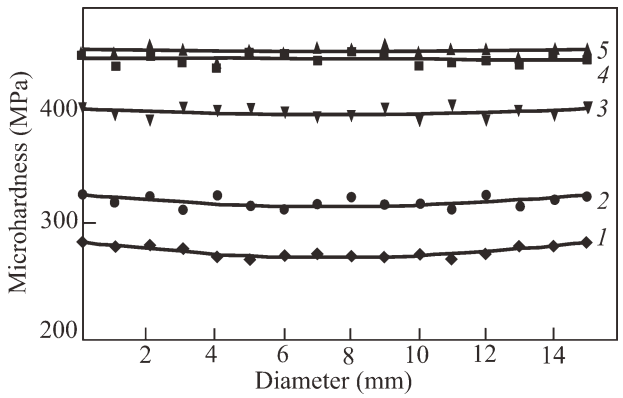

Figure 4 Microhardness distribution in the cross-section of POM extrudates: 1,2—Route C, 3–5—Route E, 1,3—ε = 4.4; 2,4—ε = 9.1; 5—ε = 11.4.

Table I contains the values of maximum extrusion pressure P_m, average values of microhardness in longitudinal section of extrudates $\bar{H}^{||}$ and cross-section $\bar{H}^{\perp}$, anisotropy of microhardness ΔH, as well as dispersion of microhardness D_H in cross-section of the samples obtained at varied deformation routes. Microhardness anisotropy is an evidence of formation of oriented structure within an extruded polymer. As the accumulated deformation ε increases, microhardness of both sections of polymer billet rises and ΔH declines. Behavior of ΔH differs from the traditional variant of solid-phase extrusion, e.g., extrusion through a conic die when ΔH increases with ε increase, too.[13] Absolute values of ΔH in the case solid state extrusion through a conic die exceed the values after ECMAE even at lower accumulated deformation. The established dependence of $\Delta H(\varepsilon)$ at ECMAE is determined by alternating-sign deformation character that forms mainly microscopic molecular orientation within extrudate.[12] The use of Route E compared to Route C yields higher absolute values of microhardness and lower anisotropy at the same accumulated deformation. At the same time, more homogeneous distribution of microhardness through the extrudate cross-section is achieved (Fig. 4). With all this going on, higher strengthening effect is obtained at lower P_m. As noted earlier, this fact can be related to lower weakening of Bauschinger's effect in the case of Route E.

Microhardness distribution over the cross-section of extrudate shows that in the case of Route C, H of peripheral areas exceeds those of the center (Fig. 4). Inhomogeneity of H distribution is related to the differences of the degree of structure reconstruction of the peripheral zone and the center. They are determined by the friction of polymer in the course of its motion through the deforming channel of the matrix.[27] The arising additional shear stresses contribute to higher strengthening of surface areas compared to the center of a billet. When Route E is realized, the divergences of absolute values of H at peripheral areas and at the center are insignificant. The increase of the accumulated deformation ε in both the cases promotes H increase and lower inhomogeneity of its distribution.

ECMAE provides not only increased density and microhardness of POM but essential improvement of elastic and strength characteristics: modulus of elasticity E, yield strength σ_y, tensile strength σ_T, measured at stretching of the samples cut along the extrusion direction (Table II). Plasticity (yield strain ε_y and strain at break ε_b) is slightly reduced here. The value of the achieved effect is determined by accumulated deformation and deformation route.

The increase of accumulated deformation ε results in increase in E, σ_y, σ_T. Nevertheless, with ε increase, the growth of these parameters becomes less significant. This behavior is characteristic of ECMAE of semicrystalline polymers,[11,12] differing from the observed behavior in the cases of such methods of solid-phase processing as die-drawn, hydrostatic extrusion, rolling with side constrains, where almost linear growth of these characteristics with accumulated deformation increase takes place.[16,17] The evolution of plasticity characteristics at ECMAE also differs from the observed values at the use of traditional schemes of solid-phase

TABLE II
Influence of ECMAE on Physical and Mechanical Properties of POM

Routes of deformation	Accumulated strain values	Density, g cm^{-3}	Modulus of elasticity	Yield strength	Tensile strength	Yield strain	Strain at break
			MPa			%	
Initial	0	1.3952	2500	54	62	7.0	25.0
Route C	4.4	1.4061	3450	128	130	5.0	19.6
	6.7	1.4100	3900	155	160	5.2	20.7
	9.1	1.4107	4050	170	182	5.3	20.8
Route E	4.4	1.4204	5075	231	240	5.9	23.4
	6.7	1.4212	5140	233	242	6.0	23.4
	9.1	1.4218	5250	238	248	6.3	23.5
	11.4	1.4220	5270	240	248	6.4	23.5

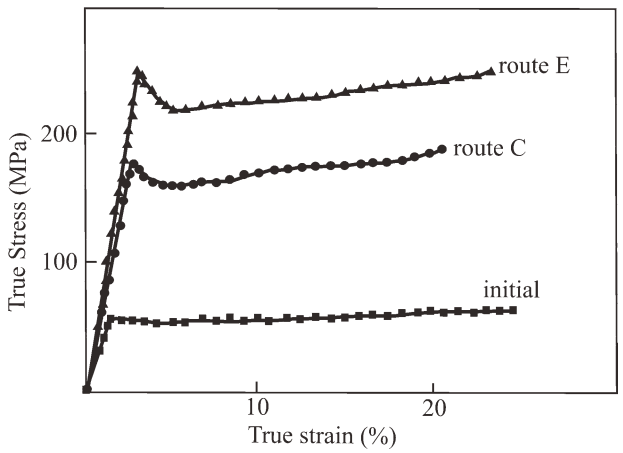

Figure 5 True stress–true strain dependencies during tensile drawing for initial POM and after ECMAE, $\varepsilon = 9.1$.

extrusion with continuous reduction of plasticity at deformation accumulation.[13,28] For ECMAE, ε_y and ε_b values reach a constant level starting from certain values of ε. The best combination of elastic, strength and plastic characteristics is observed at ECMAE, Route E. At the same time, the best set of deformation and strength characteristics is achieved at lower ε compared to Route C.

Figure 5 presents typical true stress–true strain curves of the initial POM and after ECMAE one. It is seen that ECMAE calls forth appearance of yield drop of $\sigma - \varepsilon$ curves. According to work,[29] this process is pure kinetic phenomenon without any structure reconstruction in the crystal. The height of yield drop depends on the concentration of the mobile dislocations in the sample before deformation and their ability to multiply and to "gather speed" at stress increase, and the presence of residual stresses in the sample that are realized at the maximum point and reduce the external force. The highest yield drop is observed in samples deformed by Route E, being probably connected with higher inner stress accumulated in extrudates and larger number of possible slip planes.

Increase of microhardness and strength characteristics of extruded POM can be determined by both the formation of oriented structure and increase of cristallinity degree of the samples.[30] The last fact is confirmed by the results of density measurements and DSC data (Table III). DSC curves of POM samples exposed to ECMAE demonstrate growth of onset temperature, insignificant shift of the main melting peak toward higher temperatures and the emergence of additional high-temperature melting peak (Fig. 6). In the case of extrudates obtained with using Route E, this peak was located at higher temperatures, having larger area than the samples deformed along Route C. Such behavior of the onset temperature and the top of the main melting peak can be related to the destruction of the thickest crystallites as a result of deformation and the conserved part of larger crystallites that can be even increased due to deformation-induced crystallization. The last fact is confirmed by the increase of the total enthalpy of fusion ΔH_f, which is maximum for POM processed with Route E (Table III).

Arising melting duplicate at DSC curves was pointed to in work[17] with regard to POM and other polymers, in particular, high density polyethylene[31] that was determined by formation of two types of crystal structures varying in degree of perfection of crystallites. DSC curves of POM samples subjected to ECMAE demonstrated also the reduction of peak width that can be determined by the declined dispersion of crystallite thickness. At the same time, partial increase of the thickness of crystalline stem l_c (Table III) occurs. The highest values of l_c are achieved at the processing along Route E. One can notice a small, systematic deviation of the density-based degree of crystallinity toward higher values as compared to respective values estimated from DSC data. Similar differences of crystallinity estimated from the heat of melting and density are frequently observed for many semicrystalline polymers.[32]

It is known that such structural defects as microvoids or interlamellar voids of few nanometers in size, when present in a polymer are thought to act as potential failure sites when the polymer is deformed in tension. In particular, the strength of POM, unlike the modulus, is very much influenced by morphological factors such as voids. Figure 7 presents the surfaces of brittle fracture surface of POM before and after ECMAE. Spherical porous structure is observed in the initial polymer [Fig.

TABLE III
Effect of ECMAE on Structural and Thermal Characteristics of POM

Routes of deformation	Accumulated strain values	Temperature of melting peak, T_m, K		Enthalpy of fusion, J g^{-1}	Degree of crystallinity, χ_c, from		Thickness of crystalline stem, l_c, nm
		T_{m1}	T_{m2}		DSC	Density	
Initial	0	438		170	0.52	0.58	8.9
Route C	9.1	439	440	196	0.60	0.64	9.4
Route E	9.1	439	443	218	0.67	0.69	10.4

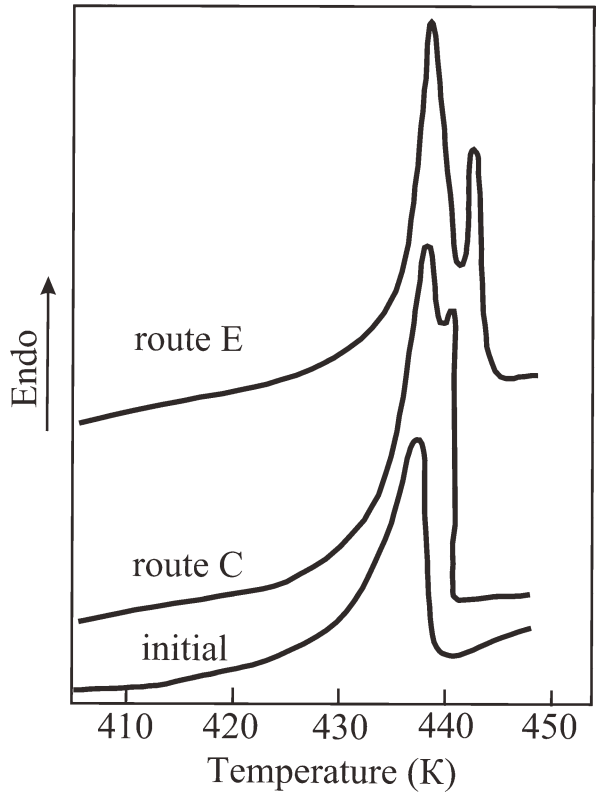

Figure 6 DSC traces for specimens of initial POM and after ECMAE,$\varepsilon = 9.1$.

7(a)]. ECMAE, Route C results in partial healing of pores in longitudinal and cross-sections of extrudates [Fig. 7(b)]. ECMAE, Route E demonstrates total pore healing [Fig. 7(c)].

Histograms of size distributions of pores illustrate this process (Fig. 8). Route C results in declined average pore size d in longitudinal and transversal sections of extrudates from 700 and 694 nm down to 278 and 272 nm, respectively. The distribution becomes narrow and is shifted toward $d \prec 500$ nm, whereas this interval of the initial POM is 100–1000 nm. In the case of Route E, starting from $\varepsilon = 4.4$, there is no visible porosity in extrudates in both the sections. It should be noted that in cases of die-drawing, hydrostatic extrusion of POM,[16] there was no actual pore healing but pores became elongated along polymer drawing direction. The characteristic ratio A determined as the ration of lengths of the major and the minor axis of pores linearly increased with the growth of accumulated deformation (degree of drawing). The void aspect ratio of the die-drawn samples is greater than the extruded samples owing to the tensile nature of the stresses in the former.[16] In the case of rolling with side constraints of POM,[17] cavities are squeezed into flat discs. The form of pores in POM subjected to ECMAE remains close to spherical and $A \approx 1$. This fact can be related to the formation of a special stress-strain state determined by alternating-sign deformation at ECMAE and the absence of significant tensile stresses. Pore healing at ECMAE correlates to the results of density measurements registering density growth at the increase of accumulated deformation ε (Table II). Maximum density increase is achieved in Route E case. This behavior differs from the observed effects in cases of die-drawing and hydrostatic extrusion,[16] where loosening of the material was registered with the increase of degree of drawing.

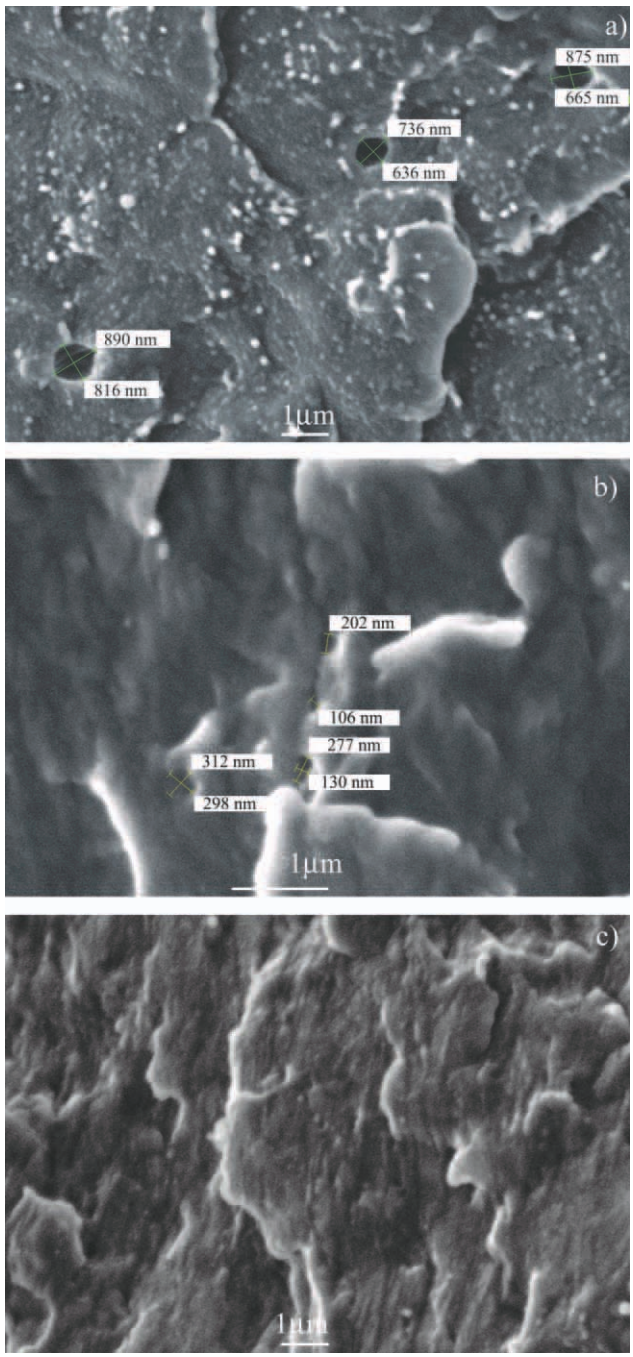

Figure 7 Microstructure of initial POM (a) and after ECMAE: (b)—Route C, (c)—Route E, $\varepsilon = 9.1$, transverse sections.

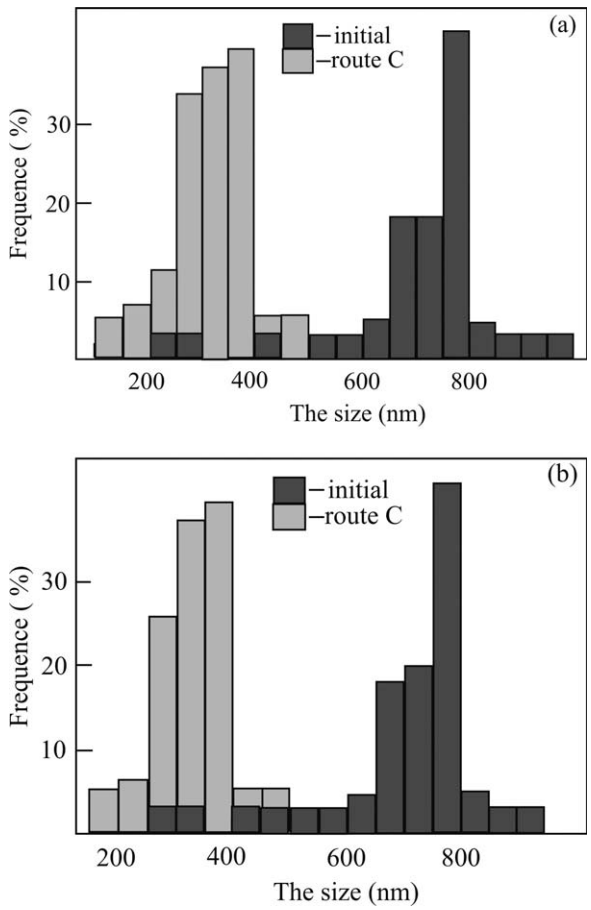

Figure 8 Histograms of the pore size distribution of initial POM and after ECMAE, Route C, $\varepsilon = 9.1$. (a)—transverse, (b)—longitudinal sections.

CONCLUSIONS

Equal channel multiple angular is an effective method of solid-phase structure modification of POM determining the increase in density, hardness and strength, low anisotropy of hardness, and yield strength at the conserved high plasticity level. The achieved result is related to the formation of oriented structure, healing of defects of the source polymer, the increase of content of the crystal phase and the degree of perfection of crystallites. The use of Route E compared to Route C allows the formation of better set of physical and mechanical properties at lower values of the accumulated deformation and extrusion pressure.

The authors express their gratitude to Dr. V.V. Burkhovetskii for assistance in SEM investigations.

References

1. Ward, I. M.; Taraiya, A. K.; Coates, P. D. In Solid Phase Processing of Polymers; Ward, I. M., Coates, P. D., Dumoulin, M. M., Eds.; Hanser: Munich, 2000; p 328.
2. Beygelzimer, Y. E.; Beloshenko, V. A. In Encyclopedia of Polymer Science and Technology; Kroschwitz, J. I., Ed.; Wiley: Hoboken, 2004; Vol. 11, p 850.
3. Segal, V. M. Mater Sci Eng A 2004, 386, 269.
4. Sue, H.-J.; Li, C. K.-Y. J Mater Sci Lett 1998, 17, 853.
5. Xia, Z.-Y.; Sue, H.-J.; Rieker, T. P. Macromolecules 2000, 33, 8746.
6. Wang, Z.-G.; Xia, Z.-Y.; Yu, Z.-Q.; Chen, E.-Q.; Sue, H.-J.; Han, C. C.; Hsiao, B. S. Macromolecules 2006, 39, 2930.
7. Phillips, A; Zhu, P.; Edward, G. Macromolecules 2006, 39, 5796.
8. Ma, J.; Simon, G. P.; Edward, G. Macromolecules 2008, 41, 409.
9. Boulahia, R.; Gloagnen, J. M.; Zairi, F.; Nait-Abdelaziz, M.; Seguela, R.; Boukharouba, T.; Lefebvre, J. M. Polymer 2009, 50, 5508.
10. Beloshenko, V. A.; Varyukhin, V. N.; Voznyak, A. V.; Voznyak, Y. V. Polym Sci A 2009, 51, 916.
11. Beloshenko, V. A.; Varyukhin, V. N.; Voznyak, A. V.; Voznyak, Y. V. Polym Eng Sci 2010, 50, 1000.
12. Beloshenko, V. A.;Varyukhin,V. N.Voznyak, A. V.; Voznyak, Y. V. Polym Eng Sci 2011, 51, 1092.
13. Beloshenko, V. A.; Voznyak, A. V.; Voznyak, Y. V. High Pres Res 2011, 31, 153.
14. Komatsu, T.; Enoki, S.; Aoshima, A. Polymer 1991, 32, 1988.
15. Komatsu, T.; Enoki, S.; Aoshima, A. Polymer 1991, 32, 2992.
16. Mohanraj, J.; Bonner, M. J.; Barton, D. C.; Ward, I. M. Polymer 2006, 47, 5897.
17. Mohanraj, J.; Morawiec, J.; Pawlak, A.; Barton, D. C.; Galeski, A.; Ward, I. M. Polymer 2008, 49, 303.
18. Baltá-Calleja, F. J. In Structure–Microhardness Correlation of Polymers and Blends; Cunha, A. M.; Fakirov, S., Eds.; Kluwer Academic Publishers: Dordrecht, 2000; p 145.
19. Flores, A.; Ania, F.; Balta-Calleja, F. J. Polymer 2009, 50, 729.
20. Haudin, J. M.; Monasse, B. In Crystallization Mechanisms an Relevant Theories; Cunha, A. M.; Fakirov, S., Eds.; Kluwer Academic Publishers: Dordrecht, 2000; p 145.
21. Sue, H.-J.; Dilan, H.; Li, C. K.-Y. Polym Eng Sci 1999, 39, 2505.
22. Chun, B. K.; Jinn, J. T.; Lee, J. K. Int J Plasticity 2002, 18, 571.
23. Campbell, B.; Edward, G. Plast Rubber Comp 1999, 28, 467.
24. Xia, Z.; Hartwig, T.; Sue, H.-J. J Macromol Sci 2004, 43B, 385.
25. Ma, J.; Simon, G. P.; Edward, G. H. Macromolecules 2008, 41, 409.
26. Wang, T.; Tang, S.; Chen, J. J Appl Polym Sci 2011, 122, 2146.
27. Enikolopyan, N. S.; Beresnev, B. I.; Myasnikov, G. D.; Prut, E. V.; Tsygankov, S. A.; Kryuchkov, A. N.; Shishkova, N. V. Dokl Phys Chem 1986, 291, 368.
28. Bartczak, Z.; Morawiec, J.; Galeski, A. J Appl Polym Sci 2002, 86, 1413.
29. Oleinik, E. F.; Rudnev, S. N.; Salamatina, O. B. Polym Sci A 2007, 49, 2107.
30. Kozlov, H. V.; Beloshenko, V. A.; Aloiev, V. Z.; Variukhin, V. N. Mater Sci 2000, 36, 98.
31. Zhorin, V. A.; Kiselev, M. R.; Roldugin, V. I. Polym Sci B 2001, 43, 1262.
32. Bartczak, Z.; Kozaneski, M. Polymer 2005, 46, 8210.